Available online at www.sciencedirect.com
ScienceDirect
Cement and Concrete Research 38 (2008) 403–412
Cement and Concrete Research

Triaxial behaviour of concrete under high stresses: Influence of the loading path on compaction and limit states

Thomas Gabet *, Yann Malécot, Laurent Daudeville

Laboratoire Sols, Solides, Structures- Risques, Université de Grenoble, CNRS, BP53, F-38041 Grenoble cedex 9, France

Received 16 March 2007; accepted 21 September 2007

Abstract

The aim of this study is to characterize the behaviour of concrete under high triaxial loading at levels of confinement and axial stress of the order of the GigaPascal. This study is carried out within a more general scope of understanding concrete behaviour under impact. The studied concrete has properties as close as possible to those used in current construction projects. A triaxial press of high capacity is used to characterize the triaxial behaviour of concrete according to various loading paths. Hydrostatic, triaxial, proportional and oedometric tests are performed and show the influence of the loading path on the compaction process. The triaxial and proportional tests show the existence of strain limit states, defining a limit states threshold independent from the loading path.

Keywords: Concrete; Experimental tests; Compression; High confinement; Loading path; GigaPascal; Triaxial; Proportional; Oedometric; Compaction; Limit states

1. Introduction

The final purpose of this study is to establish a numerical model for the prediction of the concrete response under impact. When a concrete structure undergoes a dynamic loading such an explosion or an impact, its stress state is strongly heterogeneous and time-dependent. High triaxial stress states occur, causing different damage modes which strongly depend on stress state and loading path. The phenomena of brittle damage and irreversible strain such as compaction need to be understood, and tests results at high levels of solicitations and under various loading paths need to be performed.

Numerous studies show that dynamic tests performed on concrete, for example by means of split Hopkinson pressure bars [8,19], are difficult to carry out essentially because of the brittle feature of the material that leads to a rupture in the transient stage of loading. The inhomogeneous character of the stress state in the sample, the very limited control of the loading path and the relatively poor instrumentation lead to a difficult test result analysis. The static characterization of a constitutive model to predict the dynamic behaviour is not a new practice in the study of geomaterials. Compared to dynamic tests, performing static tests allows a correct control of the loading paths and a precise measurement of strains. Thereby the strain rate effects will have to be studied too (it is a part of the global project but does not concern this specific paper). According to the literature, the rheological behaviour of concrete under compression seems to slightly depend on the strain rate for dried specimens [2,14]. The strong loading rate dependency in tension can mainly be explained by the influence of propagation velocity of defects [7].

Most of the available experimental results in literature only relates to triaxial loadings with moderate confining pressure [10]. Regarding these results the transition from a brittle to a ductile behaviour which is characteristic of cohesive materials was understood. Experimental studies on the triaxial behaviour of cementitious materials were carried out previously but they were limited to small mortar samples [1,4]. The aim of the present study is to extend this practice to "real" concretes, with aggregate dimensions of the order of one centimeter.

In this paper, tests on a low-strength plain concrete are performed, using a large capacity triaxial press named "GIGA". Stress levels overpassing one GigaPascal with homogeneous,

Abbreviations: HYD400, hydrostatic test at 400 MPa of confining pressure; TRX50; TRX650, triaxial test at 50, 650 MPa of confining pressure; PRP02; PRP035, proportional tests at $k=0.2$, $k=0.35$; UX, oedometric test.

* Corresponding author. Tel.: +33 240845684.
E-mail address: thomas.gabet@lcpc.fr (T. Gabet).

0008-8846/$ - see front matter © 2007 Elsevier Ltd. All rights reserved.
doi:10.1016/j.cemconres.2007.09.029

Nomenclature

Variables definition

ε_x, ε_θ, ε_v	axial, circumferential, volumetric strain
σ_x, σ_r	axial, radial stress
p	confining pressure
k	stress proportionality factor ($\sigma_r = k \times \sigma_x$)
$\sigma_m = (\sigma_x + 2\sigma_r)/3$	mean stress
$q = \sigma_x - \sigma_r$	principal stress difference

Sign conventions

$\sigma \geq 0$	during compression
$\varepsilon \geq 0$	during contraction

static and well controlled loading paths can be reached. A particular procedure of experimentation and instrumentation was defined. It takes into account the very high stress level and the macroporous feature of the concrete under study (Section 2). Different testing programs have been carried out: hydrostatic, triaxial, proportional and oedometric tests. Thanks to these tests, the compaction process (and the irreversible phenomena associated with) can be characterized, as well as the influence of the loading path on this compaction (Section 3). Moreover, different limit states, defining a limit state threshold independent from the loading path (Section 4) can be defined. Finally, the main perspectives for this study and the current works [17] are presented (Section 5).

2. Experimental device

2.1. The triaxial press "GIGA"

The large capacity triaxial press "GIGA" has been specifically designed and developed for this study [13]. Cylindrical concrete specimens of 7 cm in diameter and 14 cm in length can be tested at a confining pressure of up to 0.85 GPa and a maximum axial stress of 2.3 GPa. Fig. 1 shows a general scheme of the press and a section of the confining cell. The concrete specimen is placed inside this confining cell. The confining fluid, diethylhexyl azelate, a non-volatile organic liquid, is injected in the cell through the upper opening. It is then put under pressure by means of a pressure multiplier jack. The axial force is generated by means of a 10 MN jack located under the cell. The confining pressure and the axial jack displacement are controlled independently which allows different loading paths: hydrostatic, uniaxial confined (commonly named triaxial), proportional, extensional and oedometric (Fig. 2). A hydrostatic test consists of applying a pressure all around the specimen; this pressure increases linearly. During a triaxial test, the specimen is loaded axially (constant rate of displacement) while keeping the confining pressure constant. A proportional test consists of loading the specimen axially (by imposing a constant displacement rate) while keeping the pressure proportional to the axial stress ($p = k \times \sigma_x$ with $0 < k < 1$). During an oedometric test, the specimen is inserted inside a thick steel pipe to prevent radial strains. A constant displacement rate is imposed to the axial jack. The pressure all around the tube increases such that the circumferential strain is maintained to zero. This strain is measured by means of a circumferential gauge glued on the steel pipe.

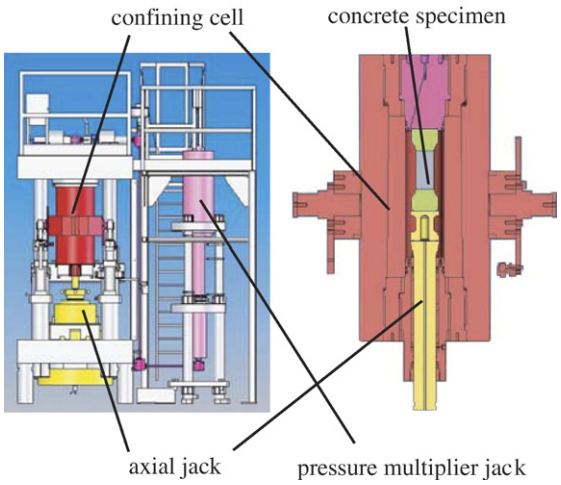

Fig. 1. General scheme of the "GIGA" press and cross-section of the confining cell.

2.2. Measurement

The concrete strain measurements are performed by means of a LVDT sensor, one axial and two circumferential gauges (Fig. 3). Gauge measurement on concrete is completely original for such levels of confinement. The LVDT sensor gives the length variation of the specimen. Each part of the LVDT is positioned on a cap, which leads to a global measurement of the axial strain[1]. By means of the axial gauge, the consistency of the signals can be checked, by giving an additional and local measurement of the strain. Since this axial gauge makes the specimen preparation for testing more complicated, it hasn't been used systematically. All

[1] In contrast to the local measurement given by the gauges.

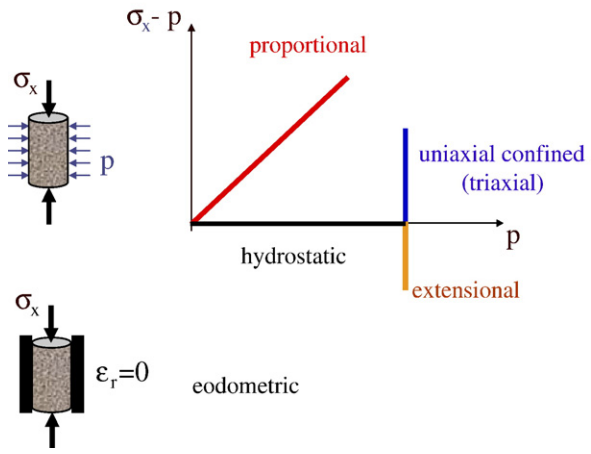

Fig. 2. Realizable loading paths on GIGA.

the axial strains presented in this paper were given by LVDT measurements. The circumferential strain is measured by means of two gauges, which are necessary because of their higher fragility and a higher variability of signals in that direction. The axial stress applied to the specimen and the pressure inside the cell are determined by means of force and pressure sensors.

The specimen lateral stress σ_r and internal radial strain ε_r during an oedometric test are both obtained from the analytical solution of a continuum mechanics calculation of a thick tube under elastic strain (Fig. 4), functions of the pressure p and considering the radial strain of the external surface of the tube is equal to zero, $\varepsilon_r(R_e)=0$.

2.3. Material and specimens

The composition and the mechanical properties of the concrete are presented in Table 1. It has a mean strength of 30 MPa in compression after 28 days and a 7 cm slump. A manufacturing procedure has been developed to be as reproducible as possible. Therefore, a minimum variability in the mechanical properties of

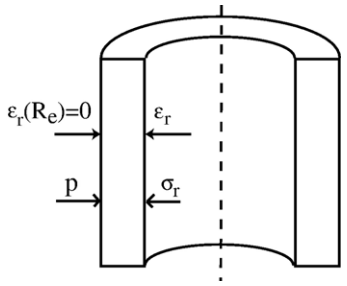

Fig. 4. Specimen lateral stress σ_r and radial strain ε_r, obtained from the analytical solution of a continuum mechanics calculation of a thick tube under elastic strain.

the concrete blocks (made at different times) is ensured. The concrete is cast in a 13.5l mould, whose base is a square of side 27 cm. The concrete block is removed 24 h after casting. The block is then kept during 28 days in a saturated environment inside waterproof bags immersed in water to insulate the concrete both physically and thermally. The block is then cored, cut and ground. During these three machining phases, water is used as a coolant and prevents specimens and tools from local overheating which could damage them. Specimens are then placed in a drying oven until the stabilization of their weight. Weight is considered as stable when its daily variation doesn't exceed 0.1% $\left(\frac{\Delta m_{24\ h}}{m} \leq 0.1\%\right)$. The influence of the degree of saturation is studied in a parallel work [17]. The weight measurement is part of a procedure to determine the porosity of the concrete specimen (porosity accessible to water) [9]. The concrete porosity, based on a measure performed on two specimens of a same concrete block, is estimated to 12%.

Note that the choice of the specimen diameter ($D=70$ mm) is a compromise between the will to test specimens under high stress levels and the necessity to keep a homogeneous structure according to the maximum aggregate size (8 mm). The specimen length ($L=140$ mm) has been determined so that the L/D ratio is equal to 2. This ratio, commonly used to characterize concrete and geomaterials behaviours, is high enough to limit the

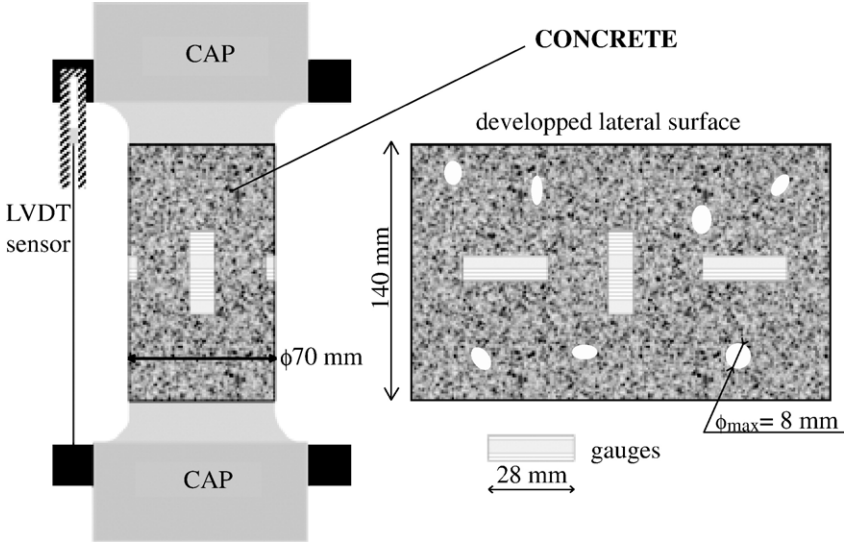

Fig. 3. Scheme of strains measurement by means of gauges and a LVDT sensor [6].

Table 1
Concrete mix proportions and characteristics

Concrete mix proportions	
Water	169 kg/m^3
Sand D (diameter)$_{max}$ 1.8 mm	838 kg/m^3
Aggregate D 0.5 to 8 mm	1007 kg/m^3
Cement CEM I 52.5 N PM ES CP2 (Vicat)	263 kg/m^3
Characteristics	
Compression strength (after 28 days)	28.6 MPa
MPa maximum size aggregate	8 mm
Concrete measured porosity	12%
Density	2.2

influence of boundary conditions on the specimen behaviour and low enough to prevent buckling [11].

2.4. Specimen preparation

A test procedure has been developed to get repeatable and reliable tests by protecting the specimen from "punching"; punching is defined as the penetration of the confining fluid into the specimen after the perforation of all the membrane layers. Punching is both due to the material porosity and to the high pressure all around the specimen. When punching occurs the material properties change because of the infiltration of the confining fluid and the gauge signals are lost because of gauges or connection wires break. This procedure consists of preparing the surfaces of the specimens and setting up the protection devices after having glued the gauges (Fig. 5).

2.4.1. Surface preparation

The surface preparation consists of opening the subjacent porosity by slightly striking the surface with a sharp object (a punch) and then filling in these opened pores with a mortar whose mechanical characteristics are close to those of concrete. Filling in pores increases membranes durability. The mortar is SIKATOP® SF 126. Once subjacent porosity is opened, proper areas on the surface can be found where pores do not seem to be present at all. Then, the gauges which should not fail due to punching can hence be glued.

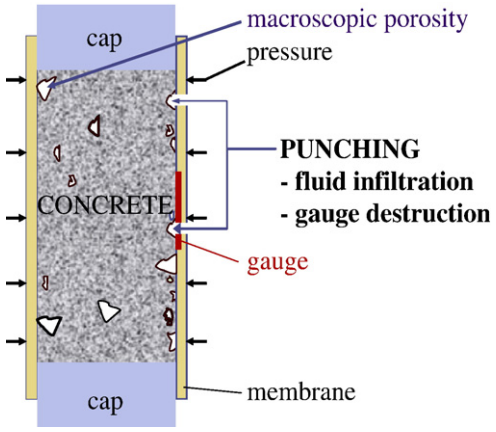

Fig. 5. Punching due to pressure and macroscopic porosity.

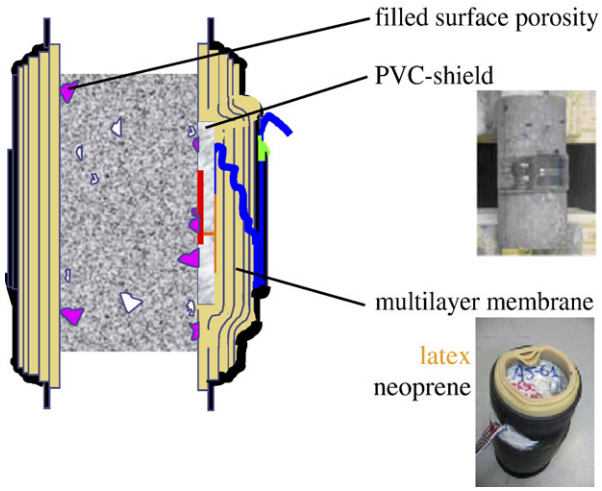

Fig. 6. Cross-section of a ready-to-test specimen, with its surface prepared, the PVC-shield and the multilayer membrane set up.

2.4.2. PVC-shield and aquaseal membrane

A PVC-shield is locally set up on gauges as an additional protection. The shield is very useful during the specimen preparation and offers a plane support surface which limits possible ruptures [16].

The specimen is then wrapped within a cylindrical membrane, which is essential to prevent the confining fluid from infiltrating the specimen. Membranes are longer than the specimen and recover a part of the caps. After different attempts using various materials (nitril, rubber, neoprene, silicon, latex), a multilayer membrane has been developed. It is made up of 8 mm of latex, used for its shear strength and its high deformability, and it is surrounded by a 1 mm neoprene layer used for its chemical inertia in order to protect the latex which can be easily damaged by the confining fluid. A cross-section of a ready-to-test specimen is presented in Fig. 6.

2.4.3. Influence of the specimen preparation on measurement

Hydrostatic tests at 700 MPa were carried out on polycarbonate specimens [16]. Results are presented on Fig. 7. The

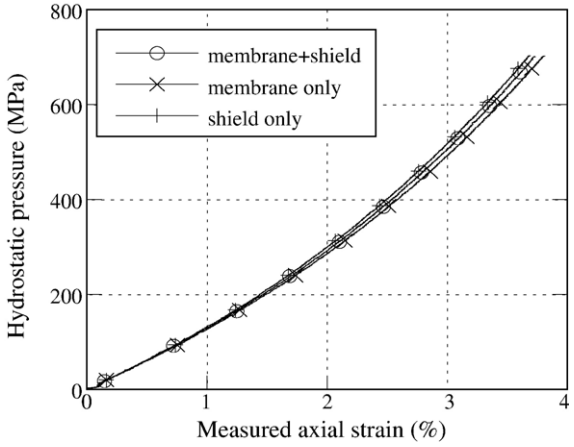

Fig. 7. Influence of the PVC-shield and the membrane on measurements: tests on polycarbonate specimen in different configurations [16].

Table 2
Test performed and presented in this paper

Tests	Loading	Block $n°$	Specimen	Dimensions ϕ[mm] × L[mm]
Hydro. cyclic	HYD400,650,650	7	A7-87	70–140
Triaxial	TRX50	4	A4-55	70–140
	TRX100	9	A9-75	70–140
	TRX200	9	A9-76	70–140
	TRX500	9	A9-72	70–140
	TRX650	7	A7-81	70–140
Proportional	PRP02	9	A9-77	70–140
	PRP03	9	A9-71	70–140
	PRP035	9	A9-79	70–140
	PRP05	9	A9-73	70–140
Oedometric		14	A14-oedo1	100–100

behaviour of this homogeneous and isotropic material is well known. It is used here as a reference to validate the measuring channels. Three tests with the membrane and PVC-shield, without the membrane and without the PVC-shield respectively have been performed, and show that the protection device has no influence on the measurement. These results confirm the ability to measure strains by means of gauges, thanks to additional protections, in spite of the high confining pressure.

3. Testing programs

Different testing programs are presented in this section. Four kinds of tests have been carried out: hydrostatic, triaxial, proportional and oedometric. The presented results are described in [6]. The tests performed and the specimens used are summarized in Table 2.

3.1. Cyclic hydrostatic tests

Three hydrostatic loadings have been performed on the same specimen at a 400, 650 and 650 MPa confining pressure (at 100 MPa/min). The loading history is presented in Fig. 8. In all the following figures, compression stresses and the corresponding contraction strains are considered as positive, whereas extensions are negative.

The results are presented in Fig. 9 in terms of volumetric behaviour, with the mean stress σ_m (equal to the confining pressure during a hydrostatic test) as a function of the volumetric strain ε_v. They show that an isotropic solicitation at high pressure leads to the development of irreversible mechanisms, which depend on the maximum stress reached during the loading history. A clear difference between the loading and unloading slopes of the HYD400 test can be observed whereas the HYD400 unloading and the first HYD650 loading curves are coincident until 400 MPa. This indicates firstly that irreversible mechanisms appear during the initial loading phase and secondly that the unloading and reloading phases until 400 MPa are elastic. During the reloading phase, once the pressure of 400 MPa is reached, the curve forks and follows a slope which corresponds to a monotonic loading. The coincidence of the first HYD650 unloading slope with the second HYD650 loading one confirms an elastic behaviour under 650 MPa of pressure if this level has already been reached.

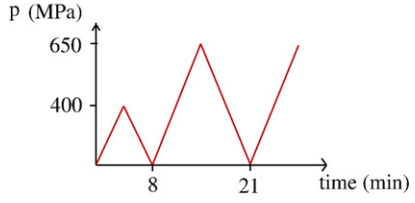

Fig. 8. Loading history of the hydrostatic test: pressure p versus time.

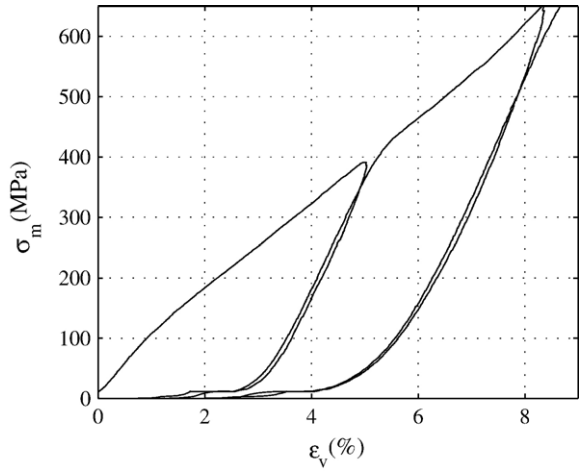

Fig. 9. Volumetric behaviour curves of cycled hydrostatic test: mean stress σ_m versus volumetric strain ε_v.

Thus, the isotropic compaction process which takes into account the influence of the loading history can be characterized. Two parallel phenomena appear simultaneously during the compaction: the structure of the material is damaging while the porosity is closing. The cohesive structure of concrete disappears progressively and is replaced by a powder structure. During the first stage of the test, the decrease of the tangent stiffness indicates an important damage just after the elastic phase. Then we observe progressively an increase of the tangent modulus which can be

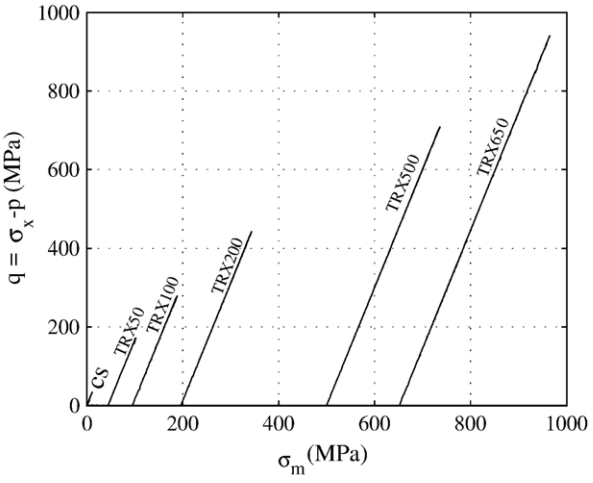

Fig. 10. Triaxial tests: loading paths in the stress space (σ_m, q).

explained by the increase of the material density due to the collapse of the porosity. These results are similar to those found in the literature for mortar [3,12,18].

3.2. Triaxial testing program

A triaxial test consists in applying a hydrostatic pressure all around the specimen up to a pressure value p (at 100 MPa/min). A constant displacement rate (5 μm/s) of the axial jack at a constant confining pressure p on the lateral face is then imposed.

Five triaxial tests have been performed with the following confining pressures: 50, 100, 200, 500 and 650 MPa. A uniaxial compression test (which is a triaxial test without confining pressure) is also presented to give an idea of the stress levels concerned with this study. The loading paths are presented in the stress space (σ_m,q) in Fig. 10.

3.2.1. Stress versus strain behaviour

The results are presented as stress/strain components curves in Fig. 11(a) and Fig. 11(b). For each confining pressure, the axial stress σ_x versus the axial strain ε_x and the circumferential strain ε_θ are plotted in Fig. 11(a). In Fig. 11(b), the principal stress difference q versus the axial strain ε_x and the circumferential strain ε_θ are plotted. Each curve is offset such that strain is equal to zero when q is equal to zero.

As we could expect, the load-carrying capacity of concrete increases significantly with the increase of the confining pressure. During the hydrostatic stage of the tests, the axial and the circumferential strains, obtained respectively with the LVDT sensor and a circumferential gauge, are very similar. Hence it can be concluded that the material is isotropic (identical axial and circumferential strains under hydrostatic loading), that the stress state is homogeneous (identical global and local signals) and that the material is reproducible (the specimens come from different concrete blocks). In this hydrostatic stage and for each test, the compaction process can be observed. The slope of the volumetric behaviour curve first decreases and then increases, due to the relative importance of the two irreversible processes observed during concrete compaction, as it has been observed during the hydrostatic tests.

During the axial loading phase at a constant confining pressure, the slope of the stress/strains curve decreases in a monotonous way with the increase of the deviatoric stress. For the 50 MPa confinement test, a peak load is reached at 200 MPa and the shape of the curve is similar to the one observed with a simple compression test. For the 100 MPa and 200 MPa confinement tests, the curves seem to tend toward a plateau. The other two tests do not exhibit any reached maximum stress. Note that the axial stress reaches a level of 1.6 GPa. The comparison of the deviatoric phase of each test (Fig. 11(b)) shows an increase of the slope with the confining pressure. This stiffening phenomenon can be explained by an increase of the material density with the confining pressure.

3.2.2. Volumetric strain versus mean stress behaviour

The volumetric behaviour of the triaxial tests is presented in Fig. 11(c). The results are presented as mean stress σ_m versus volumetric strain ε_v curves. Note that the mean stress reached during the TRX650 test is close to 1 GPa.

A test comparison shows that all the test results follow the same volumetric behaviour curve during the hydrostatic phase. Once the axial loading phase begins, a deviation of the curves is observed. For a given mean stress, the higher the deviatoric

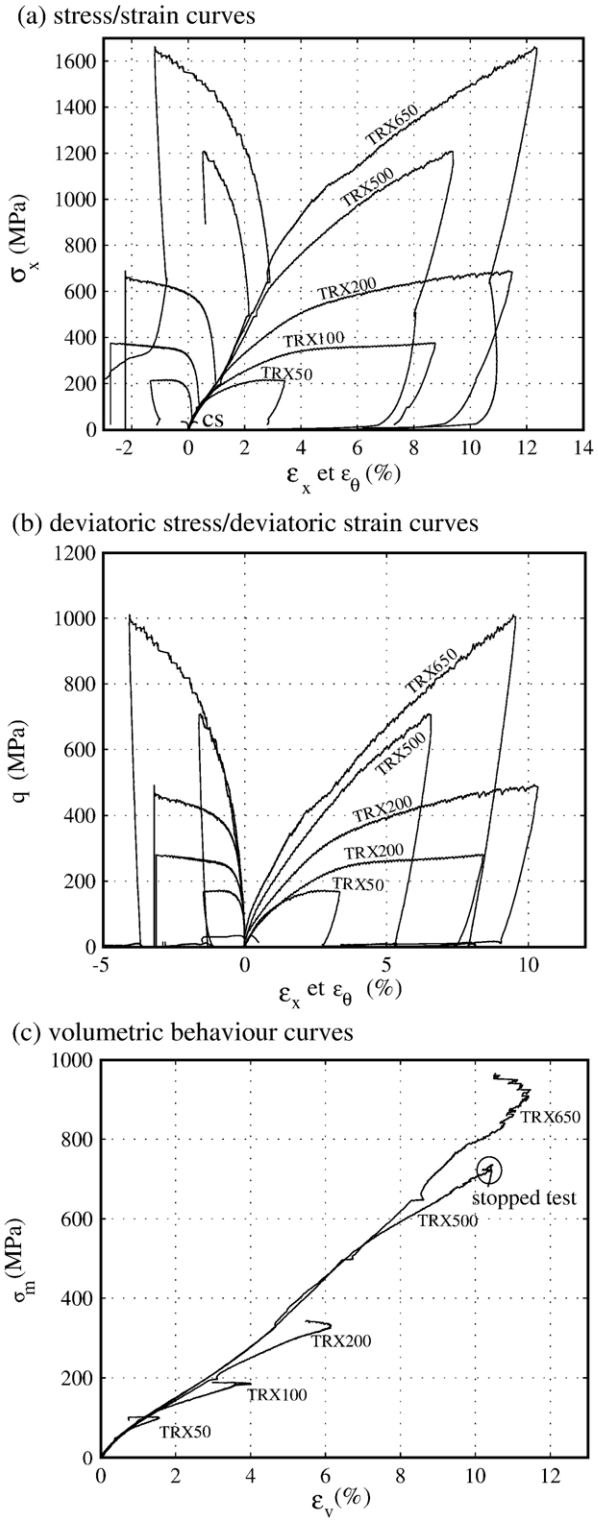

Fig. 11. Triaxial tests results.

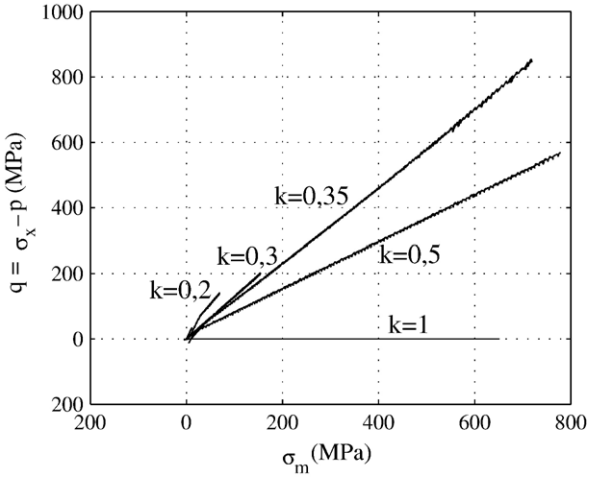

Fig. 12. Proportional tests: loading paths in the stress space (σ_m, q).

stress is, the more compacted the specimen is. It can then be concluded that shear (associated with deviatoric stress) increases the compaction.

For all the tests a limit state corresponding to a dilatancy is reached, except for the TRX500 one, which has been stopped before.

3.3. Proportional testing program

A proportional test consists of imposing the axial displacement at a constant rate (5 μm/s) while keeping the pressure proportional to the axial stress. k is the proportionality factor, with $p = k \times \sigma_x$. Four tests have been performed with k equal to 0.2, 0.3, 0.35 and 0.5. The results are compared with the results of a hydrostatic test ($k=1$) and a simple compressive one ($k=0$). The loading paths are presented in the stress space (σ_m,q) on Fig. 12.

3.3.1. Stress versus strain behaviour

For each test the axial stress is plotted as a function of both the axial strain and the circumferential strain in Fig. 13(a). The load-carrying capacity of the material increases significantly with k. For a given axial strain, both the axial stress reached and the slope increase with k. For the PRP05 test, an axial stress of 1.4 GPa has been reached. For the PRP02 test, a peak load is reached as in the simple compression test. For the PRP03 test, a slope variation can be observed. The two other tests PRP035 and PRP05 as well as the hydrostatic one do not reach any limit state.

3.3.2. Volumetric strain versus mean stress behaviour

In Fig. 13(b), the volumetric behaviour of the proportional tests is presented. The test comparison shows that for a given mean stress, a lower value of k, associated with higher deviatoric stress (and then shear stress), corresponds to a higher compaction, excepted for the PRP02 test. These results confirm that shear influences strongly the volumetric behaviour of concrete and increases the compaction process.

For the PRP02 and PRP03 tests, a limit state which corresponds to a dilatancy is reached. For the PRP035 test, a variation of the signal can be observed at the end of the test,

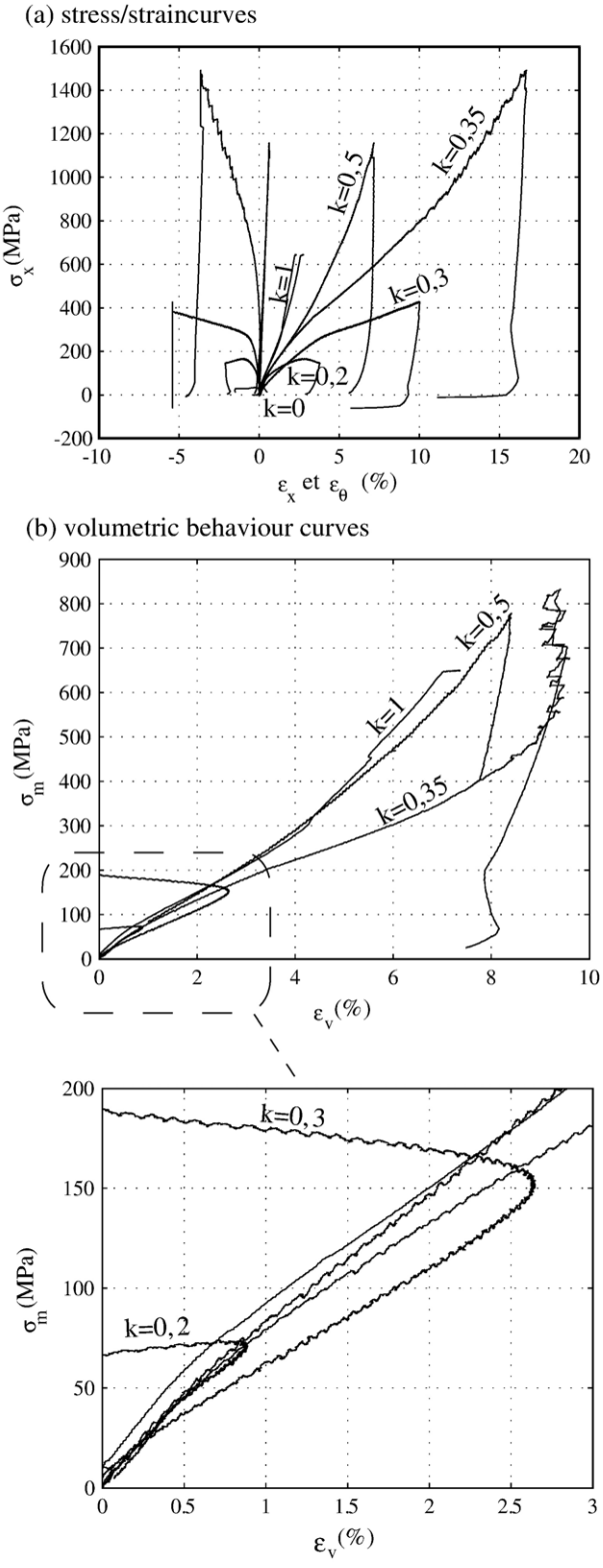

Fig. 13. Proportional tests results.

corresponding to an increase of the mean stress at constant strain. During the PRP05 test no limit state has been reached. The PRP035 and PRP05 tests behave like the hydrostatic one, with a softening followed by a hardening of the behaviour (Section 3.1). For this proportionality ratio, the lateral stress applied on the specimens is high enough to limit the lateral extensions, when at the same time, the material is compacting axially, collapsing the porosity and then increasing the density of the structure.

3.4. Oedometric test results and comparison with proportional tests results

3.4.1. Loading path

The loading path of an oedometric test is presented in the stress space in Fig. 14(a). At the beginning of the test ($0<q<50$ MPa), the curve presents a linear elastic phase, which may correspond to a phase of loading without lateral confinement. This can be explained by a small gap between the concrete specimen and the steel tube. At 700 MPa of confining pressure a sudden compaction and/or a granular restructuration may explain the slight loading accident. The test is stopped at 750 MPa of confining pressure to respect the operational limits imposed by the GIGA device.

This test is characterized by an unloading path different from the loading path, with a stiffer slope during the unloading phase. At the end of this unloading phase, the specimen reaches a hydrostatic state at 400 MPa of confining pressure. Then an extension phase begins, associated with a negative principal stress difference. The test is stopped when the specimen is in extension state.

The loading path of the oedometric and proportional tests is compared in Fig. 14(a). Thus, we can observe that the loading path of the oedometric test is close to a proportional one. The proportionality ratio would be $k=0.3$ at the beginning of the test and closer to $k=0.5$ at the end.

3.4.2. Stress versus strain behaviour

In Fig. 14(b), the axial stress is plotted as a function of the axial and radial strains. On the axial strain curve, a decrease of the tangent stiffness modulus can be observed, followed by an inflexion point and an increase of the tangent modulus. The axial strain is much more important than the radial one since the strain state is quasi-uniaxial. At the end of the unloading, irreversible strains occur.

The comparison between the oedometric and proportional test curves in Fig. 14(b) shows the same trend to those previously presented: the oedometric test behaves like a proportional test whose proportionality ratio would increase with the mean stress.

3.4.3. Volumetric strain versus mean stress behaviour

The volumetric behaviour curve is presented in Fig. 14(c). We can first notice that the mean stress reached is close to 1 GPa and that a volumetric strain of 12% has been reached during this test, which almost corresponds to the concrete porosity. Such levels of strain and stress are original for concrete and for specimens of this size (cf Table 2).

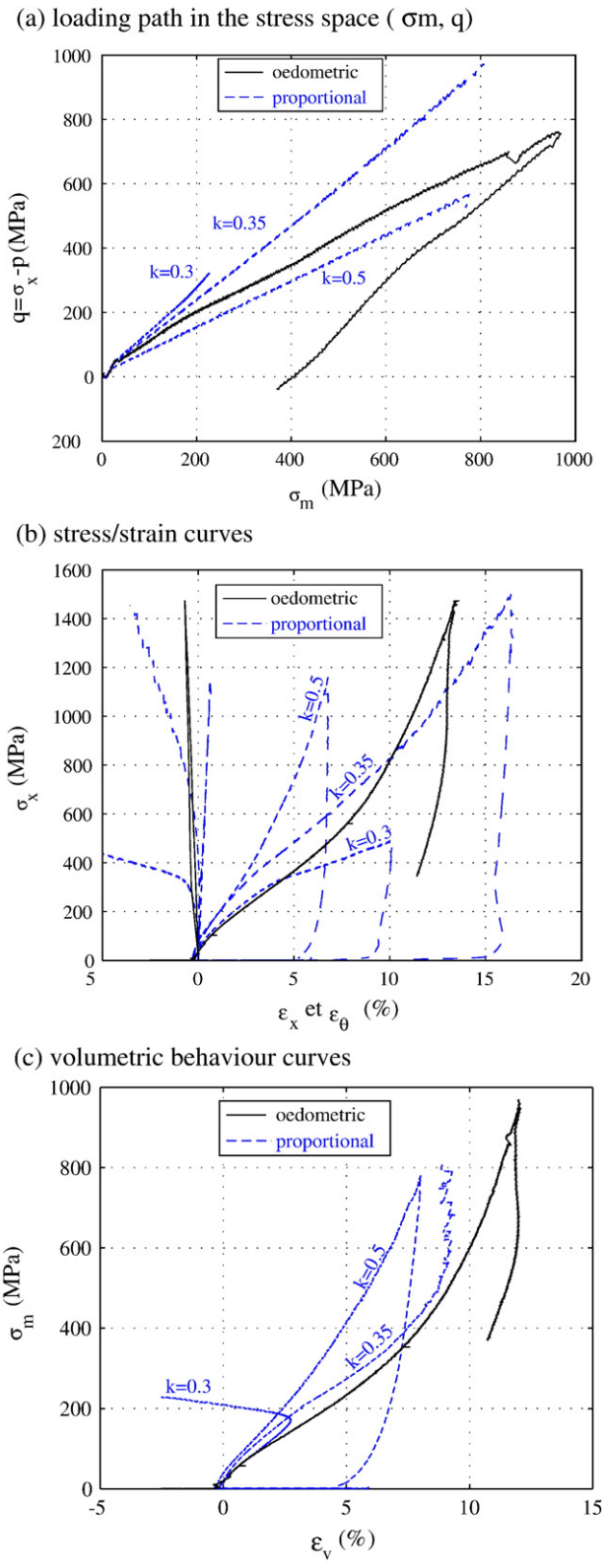

Fig. 14. Oedometric test results and comparison with proportional test results.

This test presents characteristics similar to those obtained for other oedometric tests on concrete and mortar [3]. At the end of the loading phase the slope is very stiff. The porosity collapse can explain this important stiffness.

3.5. Discussion on the influence of the loading path on the concrete behaviour

The presented tests have covered a large domain of loading paths. The influence of the loading history is shown thanks to the cycled hydrostatic tests. The influence of the confining pressure on the axial behaviour of concrete is revealed by means of the triaxial tests. The triaxial, proportional and oedometric tests show the combined influence of both the mean stress and the principal stress difference on the volumetric behaviour of concrete and more precisely the increase of the compaction process under shear stress.

The compaction curves mainly result both from a coupling between an elastic behaviour and two irreversible phenomena appearing simultaneously: the porosity collapse and the structural decohesion of the cement matrix. The strong influence of shear can mainly be explained by the generation of a relative displacement of grains inside the cement matrix due to shear stress, which causes a granular rearrangement inside the structure and makes it more compact.

4. Limit states

4.1. Stress limit states and strain limit states

Although the most common limit state is associated to the peak stress, in this study, the tests with the highest levels of confinement have not shown any stress peak. However, a transition contraction–dilatancy is frequently observed on the triaxial and proportional test curves. Thus it has been decided to compare the limit states associated with the transition contraction–dilatancy. Note that for the lowest confining pressures (CS, TRX50, TRX100 and PRP02), the transition contraction–dilatancy coincides with a stress peak.

Every limit state has been plotted in the stress space (σ_m, q). The results are presented in Fig. 15. All the triaxial tests present a transition contraction–dilatancy, except the TRX500 test, which has been stopped before. The PRP02 and PRP03 tests show a clear transition too, but for the PRP035 one, the limit state corresponds to a slope variation, and not to a clear transition.

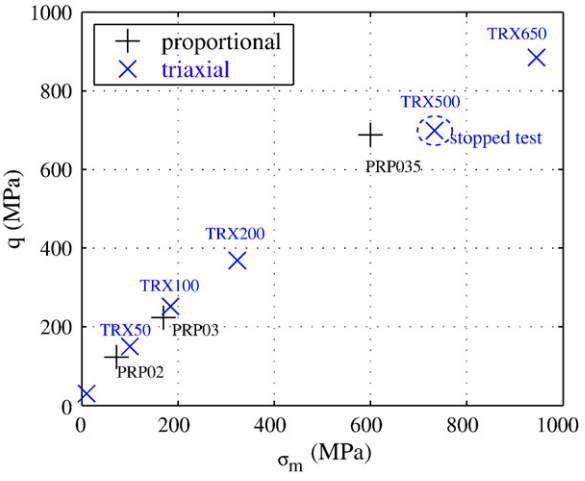

Fig. 15. Limit states points defined as transitions contraction–dilatancy on the volumetric behaviour curves of the triaxial and proportional tests, plotted in the stress space (σ_m, q).

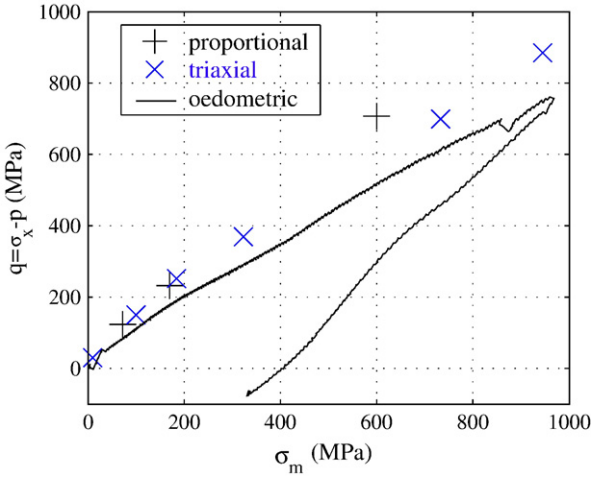

Fig. 16. The oedometric test which is never dilatant, keeps its loading path under the limit state curve, defined as a transition contraction–dilatancy.

We observe on this figure that the limit state threshold characterized by these limit state points does not seem to depend on the loading path, contrarily to the compaction process. In the lower part of the stress space, the curve displays a linear evolution. At higher mean stress a slight curvature can be observed. We can notice that the point corresponding to the maximum stress reached during the TRX500 test remains below the limit state curve, which is coherent with the fact that no transition contraction–dilatancy has been reached.

4.2. Oedometric stress path and strain limit states

The oedometric stress path is represented in the stress space (σ_m, q) and compared to the limit state points. This comparison is presented in Fig. 16. The oedometric test remains below the limit state threshold and never crosses it. This fact is coherent with the absence of dilatancy during such a test.

Although the loading path is just below the limit state curve, this test generates the most important volumetric strains. Paradoxically, for a given mean stress, the most important compaction occurs for a loading path close to the dilatancy threshold. The granular rearrangement can explain this behaviour. Indeed, we can imagine that this rearrangement of grains inside the cement matrix makes the material more compact until a local optimum[2], corresponding with the limit state curve. Overpassing this local optimum leads to a dilatancy of the material.

5. Conclusion and perspectives

Thanks to a protocol to prepare the specimens, high pressure tests have been performed on a low-strength concrete,

[2] This optimum is considered as local because it depends on the loading state. Therefore, it can certainly be associated with the limit state curve and not only a single point.

with strains measured by means of gauges despite the macroscopic porosity. A multilayer membrane and a specific surface preparation have been developed to protect the specimens and the gauges from punching. The consistency of the results during the hydrostatic phase of the triaxial tests has put in evidence a specimen isotropy, a stress homogeneity and a good reproducibility.

Hydrostatic, triaxial, proportional and oedometric tests have been performed on dried plain concrete specimens. Levels of confinement of the order of the GigaPascal, axial stress of 1.6 GPa and volumetric strains of 12% have been reached during these tests. The results of these tests have revealed an influence of the loading path on the compaction behaviour which confirms previous studies carried out on mortar specimens. Thanks to cyclic hydrostatic tests, the compaction process has been described. Regarding to the triaxial, proportional and oedometric test results, it has been proved that the deviatoric stress, associated to shear stress increases the compaction process. This sensitivity to the deviatoric stress can be explained by a granular rearrangement inside the matrix under shear stress.

Plotting the limit states reached during the triaxial and proportional tests in the (σ_m, q) space has allowed to define a threshold independent from the loading path. Hence, even if the compaction behaviour depends on loading path, the limit state does not. The most important levels of stress and strain have been reached during the oedometric test. It has brought the idea that the most important compaction at given mean stress was paradoxically obtained at the limit of dilatancy.

This experimental study is still in progress. Others loading paths are being studied. Extension tests will be soon performed to show the possible influence of the Lode angle on the material behaviour. Parallel studies are being carried out in order to evaluate the influence of the water content of the specimens on the material response. Tests at different degrees of saturation are being performed and compared with the tests presented in this paper [17] to show the influence of water on concrete behaviour and limit state curves. Other concrete mix proportions are also studied in order to show their influence on the concrete response [15] (soon to be published).

Acknowledgment

The GIGA press was implemented in Laboratoire 3S in the framework of a cooperation agreement with the Délégation Générale pour l'Armement (DGA, French Ministry of Defense). This research has been developed with the financial support of the Centre d'Etudes Techniques de Gramat (CEG, DGA) [5]. We would like to thank Dr. Eric Buzaud (CEG) for giving technical and scientific advice.

References

[1] Z. Bazant, F. Bishop, T. Chang, Confined compression tests of cement paste and concrete up to 300 ksi, ACI Journal 33 (1986) 553–560.
[2] P. Bischoff, S. Perry, Compressive behaviour of concrete at high strain rates, Materials and Structures 24 (1991) 425–450.
[3] N. Burlion, Compaction des bétons: éléments de modélisation et caractérisation expérimentale. PhD thesis, ENS Cachan, France, 1997.
[4] N. Burlion, G. Pijaudier-Cabot, N. Dahan, Experimental analysis of compaction of concrete and mortar, International Journal for Numerical and Analytical Methods in Geomechanics 25 (2001) 1467–1486.
[5] DGA, Projet d'étude amont 000701: Modèles matériaux pour simulation en dynamique rapide- thème béton, 2002. Beginning: December 2002, Client: DGA/STTC, Duration: 4 years, Cost: 1.7 M euro.
[6] T. Gabet, Comportement triaxial du béton sous fortes contraintes: Influence du trajet de chargement. PhD thesis, Université Joseph Fourier, France, 2006.
[7] F. Hild, C. Denoual, P. Forquin, X. Brajer, On the probabilistic-deterministic transition involved in a fragmentation process of brittle materials strains, Computers and Structures 81 (12) (2003) 1241–1254.
[8] B. Hopkinson, A method of measuring the pressure in the deformation of high explosives or by the impact of bullets, Philosophical Transactions of the Royal Society A213 (1914) 437–452.
[9] ISO-5017, Dense Shaped Refractory Products — Determination of Bulk Density, Apparent Porosity and True Porosity, 1998.
[10] H. Li, D. Pugh, Mechanical Behaviour of Materials Under Pressure, Elsevier, 1970.
[11] A.M. Neville, Propriétés des bétons, Eyrolles, 2000.
[12] J.M. Schmidt, High pressure and high strain rate behaviour of cementitious materials: experiments and elastic/vicoplastic modeling. PhD thesis, University of Florida, USA, 2003.
[13] Thiot, Thiot-ingénierie, 2004. la Croix Blanche 46130 Saint Michel Loubejou, France.
[14] F. Toutlemonde, Résistance au choc des structures en béton; du comportement du matériau au calcul des ouvrages. PhD thesis, ENPC, 1995.
[15] X.H. Vu, Influence du degré de saturation et du rapport E/C du bé tonsur son comportement sous fort confinement. PhD thesis, École Doctorale Mécanique et 2007. Énergétique, Université Joseph Fourier, Laboratoire 3S., 2007.
[16] X.H. Vu, T. Gabet, Y. Malécot, L. Daudeville, Experimental analysis of concrete behavior under severe triaxial loading, The 2005 Joint ASCE/ASME/SES Conference on Mechanics and Materials, Mc-Mat 2005 Mechanics and Materials Conference Baton Rouge, Louisiana, Jun 2005.
[17] X.H. Vu, Y. Malécot, L. Daudeville, A first analysis of concrete behaviour under high confinement: influence of moisture content, In First Euro Mediterranean Symposium in Advances on Geomaterials and Structures, Tunisia, May 3–5 2006.
[18] T. Warren, A. Fossum, D. Frew, Penetration into low-strength (23 mpa) concrete: target characterization and simulations, International Journal of Impact Engineering 30 (2004) 477–503.
[19] H. Zhao, G. Gary, On the use of shpb techniques to determine the dynamic behavior of materials in the range of small strains, International Journal of Solids and Structures 33 (23) (September 13 1996) 3363–3375.